JMEPEG (2014) 23:3842–3848
DOI: 10.1007/s11665-014-1186-2
©ASM International
1059-9495/$19.00

Effect of Aging Treatments on the Mechanical and Corrosive Behaviors of Spray-Formed 7075 Alloy

Rui-ming Su, Ying-dong Qu, and Rong-de Li

(Submitted September 2, 2013; in revised form July 16, 2014; published online August 14, 2014)

Mechanical properties, microstructure, exfoliation corrosion (EXCO), and intergranular corrosion (IGC) behaviors of the spray-formed 7075 aluminum alloy after T6, T73, retrogression (R), and re-aging (RRA) treatment, respectively, were studied by using tensile tester, transmission electron microscope, and scanning electron microscope. The results show that the T6 process can increase the ultimate tensile strength (UTS) up to 760 MPa, while it decreases the elongation, the EXCO, and the IGC resistance of the alloy. The T73 process can improve elongation, the EXCO, and the IGC resistance of the alloy. The corrosion resistance of the alloy can also be improved by R and RRA processes with retrogression times increase. The tiny precipitated phases distributed homogeneously in the matrix can increase the UTS. The close-connected discrete grain boundary phases (GBP) and the narrow precipitate free zones (PFZ) will lower the elongation, the EXCO, and the IGC resistance of the alloy. Contrarily, the discrete GBP and wide PFZ can improve the elongation, the EXCO, and the IGC resistance of the alloy. The EXCO and the IGC behaviors for the spray-formed 7075 alloy after different aging treatments have been established according to the standards of ASTM G34-2001 (2007) and ASTM G110-1992 (2009).

Keywords 7075 aluminum alloy, exfoliation corrosion, intergranular corrosion, retrogression and re-aging, spray forming

1. Introduction

The 7075 (Al-Zn-Mg-Cu) alloy has been widely used in the aerospace industry due to its desirable mechanical properties (Ref 1) with the general acceptable tensile strengths between 510 and 530 MPa (Ref 2, 3). In order to further improve the mechanical properties, the spray-formed method is used and the strength over 730 MPa (Ref 4-6) was obtained for 7075 alloy.

However, local corrosion, including pitting corrosion, crevice corrosion, intergranular corrosion (IGC), exfoliation corrosion (EXCO), etc., usually occurs for 7xxx series aluminum alloys. Especially, EXCO and IGC are obviously harmful, which will result in the strength and plasticity of the material to decrease significantly (Ref 7). Therefore, the corrosion mechanism investigations are very important for improving the corrosive properties of the alloy. The widely acceptable mechanism for the EXCO was suggested by Kelly and Robinson (Ref 8-11). The Reboul's theory (Ref 12) also explained the EXCO phenomena. Furthermore, the mechanism for the IGC has now become a hot topic for scientists and three important theories were suggested (Ref 13-17).

Rui-ming Su, Ying-dong Qu, and **Rong-de Li,** School of Materials Science and Engineering, Shenyang University of Technology, Shenliaoxilu 111, Shenyang Economic and Technological Development Area, Shenyang 110870, Liaoning, China. Contact e-mails: suruiming1984@gmail.com and quyingdong@163.com.

The effect of heat treatment on the properties of the EXCO and the IGC for 7xxx series aluminum alloy prepared by using traditional casting process was also reported (Ref 18-22). However, few papers involved in the EXCO and the IGC resistance for spray-formed alloy were reported even if they involved the effect of aging treatment on the mechanical properties for spray-formed alloy (Ref 23-30). It has been shown that the RRA process can improve corrosion resistance to levels approaching those of the T73 condition. Therefore, the studies of the RRA treatment on the microstructure and corrosion resistance for spray-formed 7075 alloy were spontaneously chosen as a subject to investigate. So this paper is studied on the effect of RRA treatment on microstructure, intergranular, and EXCO behavior of spray-formed 7075 alloy. The results were discussed and compared with those obtained by T6 and T73 treatments.

2. Experimental

The 7075 aluminum alloy with alloying elements of 5.48 wt.% Zn, 2.21 wt.% Mg, 1.48 wt.% Cu, 0.189 wt.% Cr, 0.371 wt.% Fe, and 0.121 wt.% Si was sprayed with atomization gas of nitrogen (N_2), spray distance of 370-380 mm, substrate eccentricity of 60-65 mm, conduit bore of 3.6 mm, incidence angle of 37-39°, spray temperature of 770-780 °C, crucible temperature of 735-745 °C, horizontal velocity of 0.15 mm/s, and vertical velocity of 0.18 mm/s. Then resulting bar was extruded at temperature of 400 °C, ratios of 30:1 and feeding rate of 1.5 mm/s.

The test samples were cut from the as-extruded bar for the two-stage solid solution, i.e., 450 °C for 1 h and 475 °C for 2 h, respectively, after which the samples were water quenched to room temperature. The details of aging treatments are listed in Table 1.

Table 1 Aging treatment conditions

Aging treatments	Conditions
T6	120 °C × 24 h
T73	120 °C × 8 h + 160 °C × 16 h
R1	120 °C × 24 h + 200 °C × 5 min
R2	120 °C × 24 h + 200 °C × 10 min
R3	120 °C × 24 h + 200 °C × 15 min
RRA1	120 °C × 24 h + 200 °C × 5 min + 120 °C × 24 h
RRA2	120 °C × 24 h + 200 °C × 10 min + 120 °C × 24 h
RRA3	120 °C × 24 h + 200 °C × 15 min + 120 °C × 24 h

According to the standard test method for EXCO susceptibility in 2XXX and 7XXX series aluminum alloys (ASTM G34-2001), the EXCO solution contains NaCl, KNO_3, and HNO_3 with concentration of 4.0, 0.5, and 0.1 mol/L, respectively, in the distilled water. The temperature and time for the specimens immersed in the solution are 25 ± 3 °C for 48 h, respectively. The ratings for the EXCO were established according to the standard photographs N (no appreciable attack, surface can be disrobed, or superficially etched), P (pitting; discrete pits, sometimes with a tendency for undercutting and slight lifting of metal at the pit edges), and EA to ED (exfoliation; EA to ED represent the EXCO becoming more and more seriously).

The standard of ASTM G110-1992 (2009) is referred to evaluate the IGC resistance of heat treatable aluminum alloys by immersion in a solution with 57 g of sodium chloride and 10 mL of hydrogen peroxide, respectively, in a 1 L distilled water. The specimen in the solution was maintained for 6 h at temperature of 30 ± 3 °C. The un-etched polished surfaces were examined by S-3400N scanning electron microscope (SEM) made by Hitachi with 500 magnifications.

The microstructures for the samples after different aging treatments were observed by JEM-2100 transmission electron microscope (TEM) of JEOL. The tensile samples conformed to ISO 6892-1:2009 with gage length of 25 mm and diameter of 5 mm were tested by using an MTS universal tensile tester with 10^{-4} s^{-1} of strain rate.

3. Results and Discussion

3.1 Exfoliation Corrosion

Figure 1 shows the EXCO morphologies of spray-formed 7075 alloy under different aging treatments. It can be seen form Fig. 1(a) that the corrosive caused much great penetration depth for the sample after T6 treatment. According to ASTM G34-2001 (2007), the EXCO rating of the alloy after T6 treatment is ED. However, only discrete pits appear on the surface for the sample after T73 treatment as indicated in Fig. 1(b) and the EXCO rating is P. For the sample after 200 °C retrogression for 5 min (R1), the corrosive penetrates to a considerable depth into the sample, as shown in Fig. 1(c), and the EXCO rating is attributed to EC. When the retrogression time is extended to 10 min (R2), the sample surface emerges notable layering and penetration as shown in Fig. 1(d), and the EXCO rating is EB. Furthermore, the retrogression time is extended to 15 min (R3), many tiny blisters appear on surface of sample as indicated in Fig. 1(e), and the EXCO rating is EA. Figure 1(f) shows the surface with notable layering and blisters for the sample after RRA1 treatment and the EXCO rating is EB. From Fig. 1(g), it can be found that thin slivers and flakes with slight separation appear on the surface for the sample after RRA2 treatment, and the EXCO rating is EA. For the RRA3-treated sample, many discrete pits with a tendency of protruding at the pit edges can be observed on the surface as shown in Fig. 1(h), and the EXCO rating is P. Therefore it can be seen that the RRA treatment can improve EXCO resistance of the samples with time increases.

3.2 Intergranular Corrosion

Figure 2 shows the cross-sections for the samples after different aging treatments to reveal the IGC resistance of spray-formed 7075 alloy. For the T6 treatment sample, the surface is rough and uneven as shown in Fig. 2(a), which indicates that the corrosive has penetrated to a great distance of about 131.4 μm into the alloy and the IGC is serious in such case. It can be seen from Fig. 2(b) that only discrete pits appear on surface of the sample and the IGC depth is about 2.0 μm. Therefore, the alloy presents a favorable IGC resistance after T73 treatment. For the samples underwent retrogression treatment (R1-R3), the IGC depths are decreased with the retrogression time increases, as indicated in Fig. 2(c)-(e). Figure 2(c) shows the sample underwent 200 °C retrogression for 5 min (R1), the IGC is serious and the IGC depth is 96.8 μm. When the retrogression time increases to 10 min (R2), the pits become shallow and the IGC depth is 52.6 μm as shown in Fig. 2(d), which indicates that retrogression time can alleviate the IGC depth. From Fig. 2(e), it can be found that the IGC depth is only 35.6 μm. Therefore, IGC resistance is substantially improved after retrogression for 15 min (R3).

The RRA treatment can further improve the IGC resistance. Figure 2(f) shows some pits on surface of sample after RRA1 treatment. The corrosive can infiltrated into the matrix under the help of some pits and the IGC depth reaches 28.8 μm. It can be found from Fig. 2(g) that the pits on surface of sample decrease and become shallow after RRA2 treatment, and the IGC depth is reduced to 16.8 μm. However, the IGC depth is further reduced to 5.2 μm for the sample underwent RRA3 treatment, and only sporadic pits on surface are observed as indicated in Fig. 2(h). Comparison to T6 treatment, corrosion stability of alloy is observably enhanced for the alloy after RRA treatment, and comparable to those after T73 treatment. According to our experiments, the EXCO and the IGC for the spray-formed 7075 alloy after various aging treatments can be established by referring ASTM G34-2001 (2007) and ASTM G110-1992 (2009), which are shown in Table 2, including the mechanical properties of the alloy.

3.3 Mechanical Properties

The typical tensile stress-strain curves of samples after T6, T73, and RRA2 treatments are given in Fig. 3. The ultimate tensile strength (UTS), the yield strength (YS), and elongation

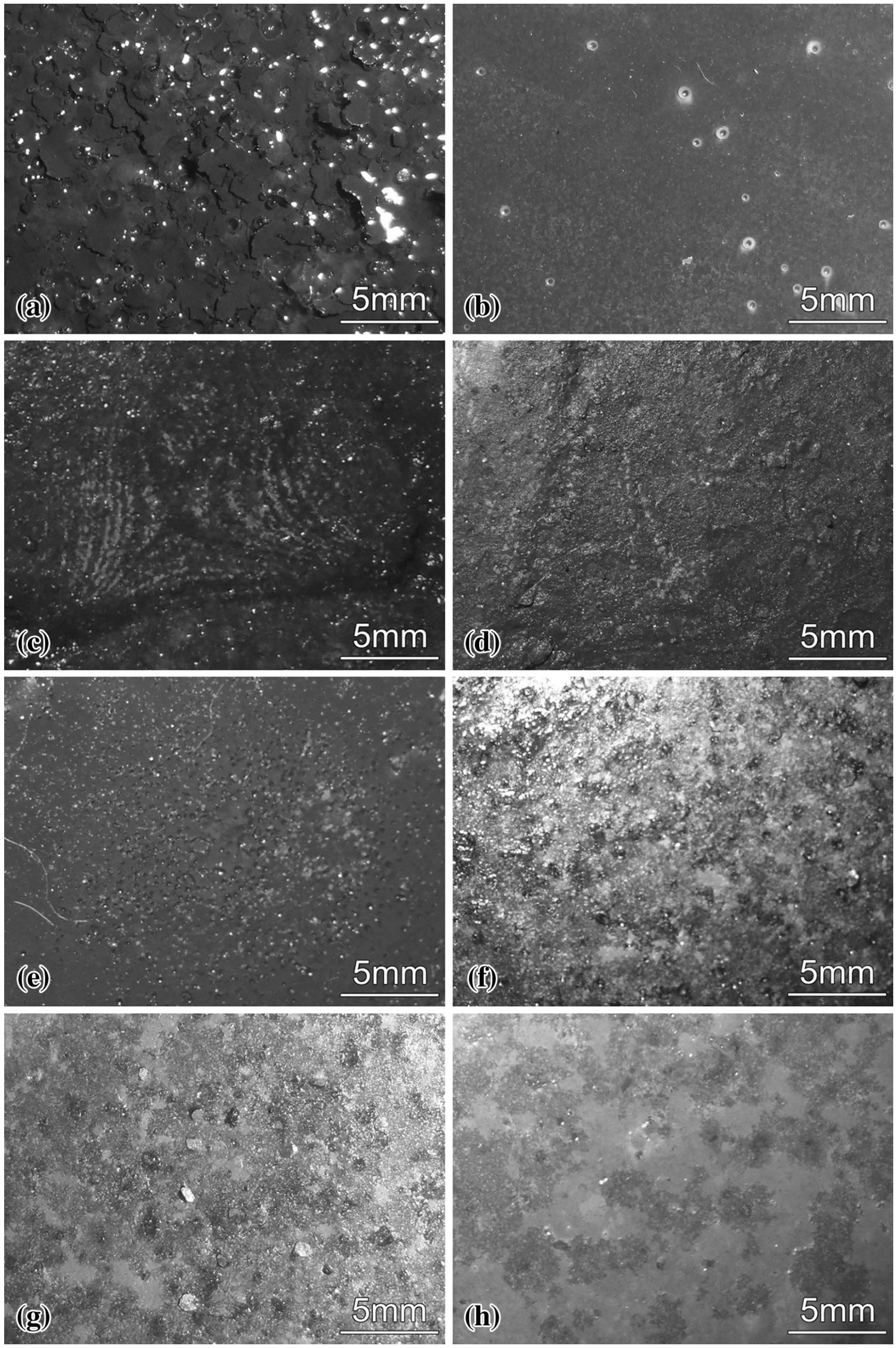

Fig. 1 Exfoliation corrosion morphologies of spray forming 7075 alloy after various aging treatments: (a) T6, (b) T73, (c) R1, (d) R2, (e) R3, (f) RRA1, (g) RRA2, and (h) RRA3

are listed in Table 2. The UTS and the elongation are 760 MPa and 4.8%, respectively, for the samples underwent T6 treatment. The UTS is reduced to 676 MPa and the elongation increases to 8.4% for the T73 treatment samples. The retrogression is the most important intermediate stage of the RRA process, which can increase the elongation of the alloy. Therefore, the elongations for all the samples treated by retrogressions are higher, while the UTSs are usually lower than those of RRA process. RRA treatments can further improve the UTSs of tested samples. We can find that the UTS (758 MPa) and the elongation (8.6%) for RRA2-treated sample are close to that for T73-treated sample.

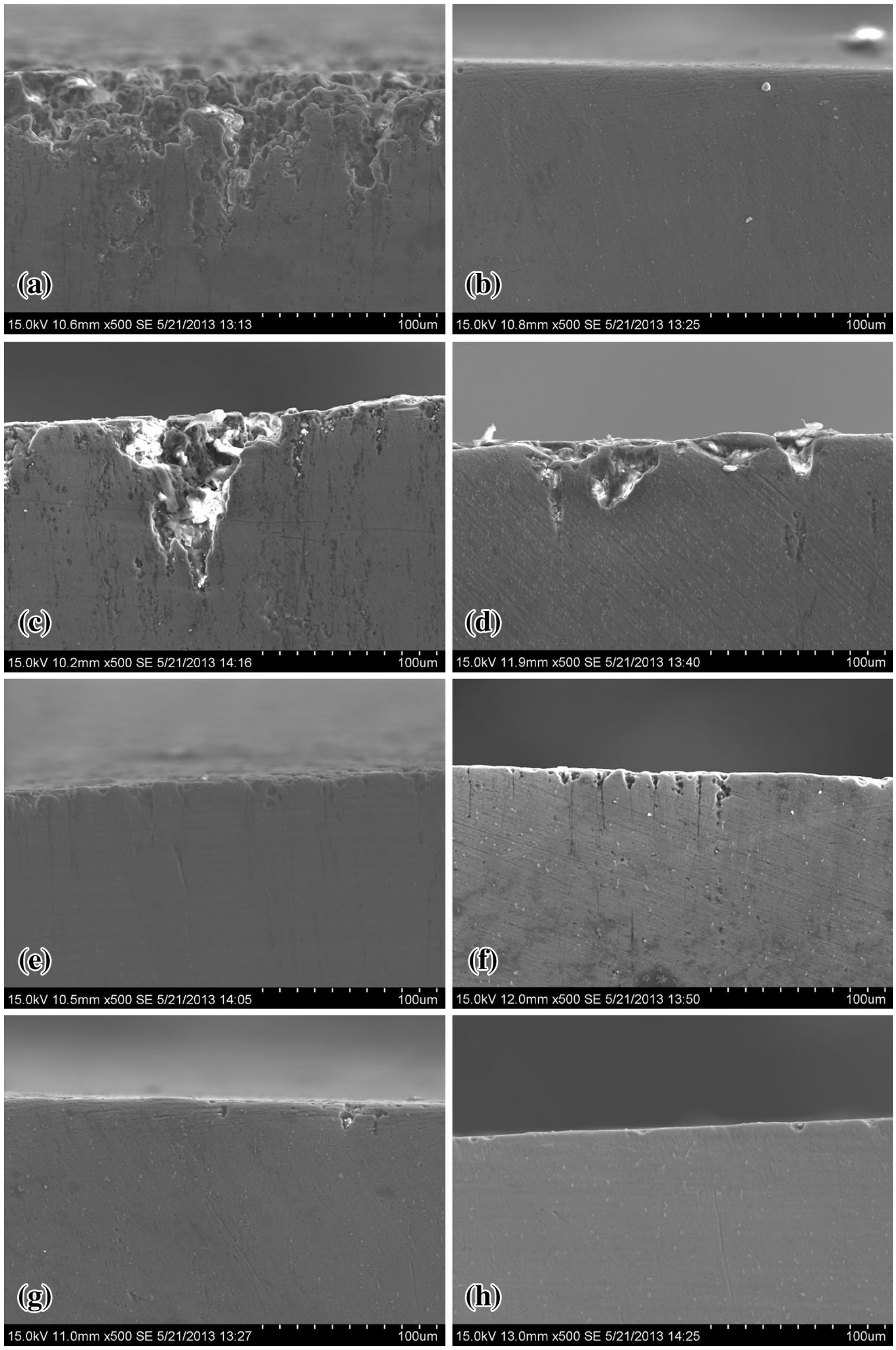

Fig. 2 SEM images of intergranular corrosion of spray forming 7075 alloy after various aging treatments: (a) T6, (b) T73, (c) R1, (d) R2, (e) R3, (f) RRA1, (g) RRA2, and (h) RRA3

3.4 Microstructure

The usual precipitation sequence of 7xxx series aluminum alloys can be summarized as super-saturated solid solution (SSSS) $\rightarrow$ GP zones $\rightarrow$ metastable η' $\rightarrow$ stable η (Ref 1). GP zones are metastable, coherent solute clusters of Zn, Mg, and Cu. The metastable η' phases, Al, Cu, and Mg components based on a solid solution of $MgZn_2$, $Mg(ZnCuAl)_2$, or $Mg(Zn_2,AlMg)$ appear as discrete platelet particles that are semi-coherent with the matrix, which is known to populate within the grains, and η is pseudostable, non-coherent of the

Table 2 Properties of spray-formed 7075 alloy after various aging treatments

Treatments	UTS, MPa	YS, MPa	Elongation, %	IGC depth, μm	EXCO rating
T6	760	719	4.8	131.4	ED
T73	676	621	8.4	2.0	P
R1	630	583	10.0	96.8	EC
R2	613	570	10.4	52.6	EB
R3	618	577	10.6	35.6	EA
RRA1	735	699	6.4	28.8	EB
RRA2	758	711	8.6	16.8	EA
RRA3	723	674	9.0	5.2	P

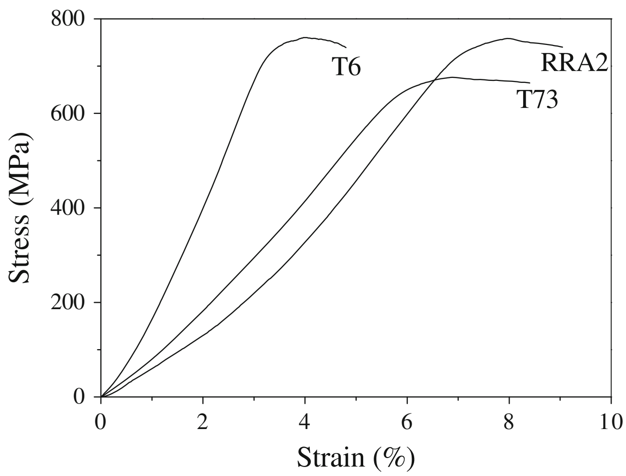

Fig. 3 Stress-strain curve of tensile samples after T6, T73, and RRA2 treatments

same phase appearing as rods or plates, which is known to populate the grain boundary.

Figure 4 shows the TEM images of spray-formed 7075 alloy after various aging treatments. From Fig. 4(a), it can be seen that abundant matrix precipitates (MPt) are thin, isolated, and dispersed for T6 sample. Sizes of these phases are 1-2 nm. At grain boundaries, grain boundary precipitates (GBP) are discrete and close-connected. The precipitate free zones (PFZ) are about 5 nm. From Fig. 4(b), it can be found that the MPt for T73 sample are bigger and more agminate than those for T6 sample. The volume fractions of the MPt are decreased and sizes are increased to 3-5 nm. At grain boundaries, the GBP become discrete and the PFZ is increased to 25 nm. The tensile strengths of the alloy are immediately influenced by the sizes and the volume fractions of the MPt. The tensile strength up to 760 MPa is obtained for the T6 sample due to abundant tiny precipitates formation in the matrix. While tensile strength is only 676 MPa for T73 sample due to the growing up of the MPt as well as its volume fractions decrease. Because the GBP are preferentially dissolved as anodes, the galvanic corrosion usually occurs in the aluminum matrix and the continuous GBP, which increases the EXCO and the IGC susceptibility of the alloy treated by T6 process. However, the discrete GBP appeared in T73 sample can obstacle to the galvanic corrosion and improve corrosion resistance of the alloy.

Figure 4(c)-(e) shows the TEM images of alloy subjected to 200 °C retrogression treatment for 5 min (R1), 10 min (R2), and 15 min (R3), respectively. It can be found that the volume fractions of the strengthening MPt in matrix are decreased and much bigger MPt can be observed for the retrogression samples. At the initial stage of retrogression treatment (R1), lots of the MPt smaller than critical size are dissolved, while a few of the MPt bigger than critical size are grew up and transformed to stable η phases, as shown in Fig. 4(c). Therefore, we can understand the reason why the strength is decreased abruptly for the R1 sample. During R2 retrogression treatment, most of the MPt are dissolved in the matrix, as shown in Fig. 4(d), the strength of the alloy is decreased to the minimum value. Subsequently, the precipitates with dispersive distribution in the matrix can increase the strength of the alloy gradually, which is shown in Fig. 4(e). The volume fractions of the precipitated phases in the matrix are obviously increased for the R3 sample. Such a phenomenon is obviously different from the 7xxx series aluminum alloys prepared by traditional casting process. It can be deduced that the MPt will be coarsened and transformed into stable phase as retrogression time increases. Therefore, the precipitated phases on grain boundaries are separated from each other, which is beneficial in improving corrosion resistance of the alloy.

For the RRA samples shown in Fig. 4(f)-(h), the tiny particles with homogeneous distribution are precipitated again in the grains. That is the reason why the strength of the alloy is increased again. The GBP on grain boundaries become thick and discontinuous with the retrogression time, i.e., the GBP are obviously coarsened and discrete distributed. Those discrete GBP, similar to those formed in T73 sample, can prevent the formation the galvanic corrosion and increase the strength of the alloy. Therefore, the RRA treatments can endow both high strength and favorable corrosion resistance for the alloy. According to the results obtained in our experiment, a wide PFZ can improve plasticity and corrosion resistance of the alloy, which is also supported by Jiang's experiment (Ref 31, 32). However, it should be noticed that the opinions about effect of PFZ on these properties are sill needed to be consistent. The Cu concentration on the corrosion resistance (Ref 33-36) after RRA and T73 treatment for Cu-containing 7075 alloy is also a reason of the favorable corrosion resistance of the alloy.

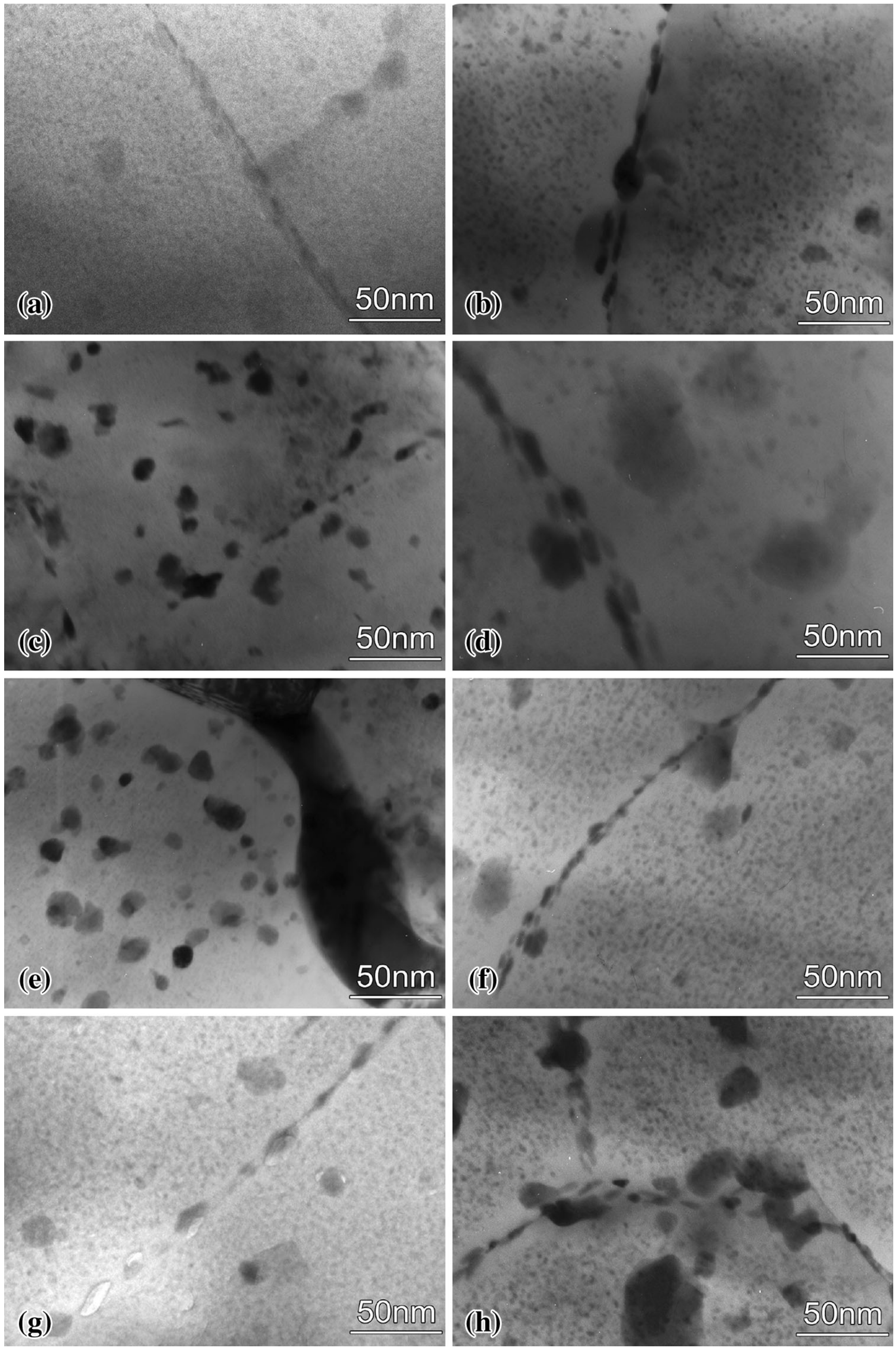

Fig. 4 TEM images of spray forming 7075 alloy after various aging treatments: (a) T6, (b) T73, (c) R1, (d) R2, (e) R3, (f) RRA1, (g) RRA2, and (h) RRA3

4. Conclusions

The EXCO and the IGC behaviors for the spray-formed 7075 alloy after different aging treatments have been established according to the standards of ASTM G34-2001 (2007) and ASTM G110-1992 (2009).

For T6 process, the UTS up to 760 MPa is obtained because the tiny MPt are homogeneously distributed in the matrix. While the close-connected discrete GBP and the narrow PFZ cause a lower elongation and the inferior EXCO and IGC susceptibility of the alloy.

For T73 process, the discrete GBP and wide PFZ can improve the elongation, the EXCO, and the IGC resistance of the alloy. However, the UTS of the alloy is reduced to 676 MPa due to the decrease of the volume fractions of the precipitates.

For retrogressing process, the MPt smaller than the critical size are dissolved, while for those of the MPt bigger than critical size will be grew up and transformed into stable phases. The corrosion resistance of the alloy can be improved with retrogression time increases.

For RRA process, the UTS up to 758 MPa is obtained because the tiny MPt are homogeneously distributed in the matrix, which is comparable to those by T6 treatment. The elongation, the EXCO rating, and the IGC depth are 8.4%, EA, and 16.8 μm, respectively, which is comparable to those obtained in T73 process.

Acknowledgments

This research was financially supported by Program for Liaoning Innovative Research Team in University (LT2012004).

References

1. G. Sha and A. Cerezo, Early-Stage Precipitation in Al-Zn-Mg-Cu Alloy (7050), *Acta Mater.*, 2004, **52**, p 4503–4516
2. S.L. George and R.D. Knutsen, Composition Segregation in Semi-solid Metal Cast AA7075 Aluminium Alloy, *J. Mater. Sci.*, 2012, **47**, p 4716–4725
3. R.E. Ricker, E.U. Lee, R. Taylor, C. Lei, B. Pregger, and E. Lipnickas, Chloride Ion Activity and Susceptibility of Al Alloys 7075-T6 and 5083-H131 to Stress Corrosion Cracking, *Metall. Mater. Trans. A*, 2013, **44**, p 1353–1364
4. R.M. Su, Y.D. Qu, R.X. Li, and R.D. Li, Study of Ageing Treatment on Spray Forming Al-Zn-Mg-Cu Alloy, *Appl. Mech. Mater.*, 2012, **217**, p 1835–1838
5. M. Jeyakumar, S. Kumar, and G.S. Gupta, Microstructure and Properties of the Spray-Formed and Extruded 7075 Al Alloy, *Mater. Manuf. Process.*, 2010, **25**, p 777–785
6. J. Fang, P.C. Wong, K.A.R. Mitchell, and T. Foster, Observations Related to the Phosphating of Aluminium Alloy 7075-T6 Using a Spraying Technique, *J. Mater. Sci.*, 1998, **33**, p 1541–1547
7. T. Ramgopal, P.I. Gouma, and G.S. Frankel, Role of Grain-Boundary Precipitates and Solute-Depleted Zone on the Intergranular Corrosion of Aluminum Alloy 7150, *Corrosion*, 2002, **58**, p 687–697
8. M.J. Robinson, The Role of Wedging Stresses in the Exfoliation Corrosion of High Strength Aluminium Alloys, *Corros. Sci.*, 1983, **23**, p 887–899
9. M.J. Robinson and N.C. Jackson, Exfoliation Corrosion of High Strength Al-Cu-Mg Alloys: Effect of Grain Structure, *Br. Corros. J.*, 1999, **34**, p 45–49
10. D.J. Kelly and M.J. Robinson, Influence of Heat Treatment and Grain Shape on Exfoliation Corrosion of Al-Li Alloy 8090, *Corrosion*, 1993, **49**, p 787–795
11. M.J. Robinson, Mathematical Modelling of Exfoliation Corrosion in High Strength Aluminium Alloys, *Corros. Sci.*, 1982, **22**, p 775–790
12. M.C. Reboul and J. Bouvaist, Exfoliation Corrosion Mechanisms in the 7020 Aluminium Alloy, *Mater. Corros.*, 1979, **30**, p 700–712
13. R.H. Brown, W.L. Fink, and M.S. Hunter, Measurement of Irreversible Potentials as a Metallurgical Research Tool, *Trans. AIME*, 1941, **143**, p 115–122
14. J.R. Galvele and S.M. de De Micheli, Mechanism of Intergranular Corrosion of Al-Cu Alloys, *Corros. Sci.*, 1970, **10**, p 795–807
15. S. Maitra and G.C. English, Mechanism of Localized Corrosion of 7075 Alloy Plate, *Metall. Trans. A*, 1981, **12**, p 535–541
16. R.G. Buchheit, J.P. Moran, and G.E. Stoner, Electrochemical Behavior of the T1 (Al2CuLi) Intermetallic Compound and Its Role in Localized Corrosion of Al-2% Li-3% Cu Alloys, *Corrosion*, 1994, **50**, p 120–130
17. R.G. Buchheit, F.D. Wall, G.E. Stoner, and J.P. Moran, Anodic Dissolution-Based Mechanism for the Rapid Cracking, Preexposure Phenomenon Demonstrated by Aluminum-Lithium-Copper Alloys, *Corrosion*, 1995, **51**, p 417–428
18. A. Conde and J. De Damborenea, Evaluation of Exfoliation Susceptibility by Means of the Electrochemical Impedance Spectroscopy, *Corros. Sci.*, 2000, **42**, p 1363–1377
19. T. Ramgopal, P.I. Gouma, and G.S. Frankel, Role of Grain-Boundary Precipitates and Solute-Depleted Zone on the Intergranular Corrosion of Aluminum Alloy 7150, *Corrosion*, 2002, **58**, p 687–697
20. L. Lin, Z. Liu, Y. Li, X. Han, and X. Chen, Effects of Severe Cold Rolling on Exfoliation Corrosion Behavior of Al-Zn-Mg-Cu-Cr Alloy, *J. Mater. Eng. Perform.*, 2012, **21**, p 1070–1075
21. J. Wloka, T. Hack, and S. Virtanen, Influence of Temper and Surface Condition on the Exfoliation Behaviour of High Strength Al-Zn-Mg-Cu Alloys, *Corros. Sci.*, 2007, **49**, p 1437–1449
22. M.J. Starink and S.C. Wang, A Model for the Yield Strength of Overaged Al-Zn-Mg-Cu Alloys, *Acta Mater.*, 2003, **51**, p 5131–5150
23. E. Salamci, Directionality in the Mechanical Properties of Spray Cast and Extruded 7xxxx Series Aluminum Alloys, *Turk. J. Eng. Environ. Sci.*, 2003, **27**, p 169–176
24. F. Wang, B. Xiong, Y. Zhang, B. Zhu, H. Liu, Z. Wang, and X. He, Microstructure and Mechanical Properties of Spray-Deposited Al-10.8Zn-2.8Mg-1.9Cu Alloy After Two-Step Aging Treatment at 110 and 150°C, *Mater. Charact.*, 2007, **58**, p 82–86
25. F. Wang, B. Xiong, Y. Zhang, B. Zhu, H. Liu, and X. He, Effect of Heat Treatment on the Microstructure and Mechanical Properties of the Spray-Deposited Al-10.8Zn-2.8Mg-1.9Cu Alloy, *Mater. Sci. Eng. A*, 2008, **486**, p 648–652
26. A.F. Oliveira, Jr., M.C. De Barros, K.R. Cardoso, and D.N. Travessa, The Effect of RRA on the Strength and SCC Resistance on AA7050 and AA7150 Aluminium Alloys, *Mater. Sci. Eng. A*, 2004, **379**, p 321–326
27. Y.H. Cai, R.G. Liang, Z.P. Su, and J.S. Zhang, Microstructure of Spray Formed Al-Zn-Mg-Cu Alloy with Mn Addition, *Trans. Nonferrous Met. Soc. China*, 2011, **21**(1), p 9–14
28. P. Lengsfeld, J.A. Juarez-Islas, W.A. Cassada, and E.J. Lavernia, Microstructure and Mechanical Behavior of Spray Deposited Zn Modified 7XXX Series Al Alloys, *Int. J. Rapid Solidif.*, 1995, **8**, p 237–265
29. E. Salamci, Ageing Behaviour of Spray Cast Al-Zn-Mg-Cu Alloys, *Turk. J. Eng. Environ. Sci.*, 2001, **25**, p 681–686
30. E. Salamci, Mechanical Properties of Spray Cast 7XXX Series Aluminum Alloys, *Turk. J. Eng. Environ. Sci.*, 2002, **26**, p 345–352
31. H. Jiang and R.G. Faulkner, Modelling of Grain Boundary Segregation, Precipitation and Precipitate-Free Zones of High Strength Aluminium Alloys—I. The Model, *Acta Mater.*, 1996, **44**, p 1857–1864
32. H. Jiang and R.G. Faulkner, Modelling of Grain Boundary Segregation, Precipitation and Precipitate-Free Zones of High Strength Aluminium Alloys—II. Application of the Models, *Acta Mater.*, 1996, **44**, p 1865–1871
33. S.P. Knight, N. Birbilis, B.C. Muddle, A.R. Trueman, and S.P. Lynch, Correlations Between Intergranular Stress Corrosion Cracking, Grain-Boundary Microchemistry, and Grain-Boundary Electrochemistry for Al-Zn-Mg-Cu Alloys, *Corros. Sci.*, 2010, **52**, p 4073–4080
34. T. Ramgopal, P. Schmutz, and G.S. Frankel, Electrochemical Behavior of Thin Film Analogs of Mg(Zn, Cu, Al)$_2$, *J. Electrochem. Soc.*, 2001, **148**, p B348–B356
35. R. Goswami, S. Lynch, N.J.H. Holroyd, S.P. Knight, and R.L. Holtz, Evolution of Grain Boundary Precipitates in Al 7075 upon Aging and Correlation with Stress Corrosion Cracking Behavior, *Metall. Mater. Trans. A*, 2013, **44**, p 1268–1278
36. D.A. Hardwick, A.W. Thompson, and I.M. Bernstein, The Effect of Copper Content and Heat Treatment on the Hydrogen Embrittlement of 7050-Type Alloys, *Corros. Sci.*, 1988, **28**, p 1127–1137